Author Manuscript

Author Manuscript

Author Manuscript

Author Manuscript

HHS Public Access

Author manuscript

J Inherit Metab Dis. Author manuscript; available in PMC 2020 May 01.

Published in final edited form as:

J Inherit Metab Dis. 2019 May ; 42(3): 470–479. doi:10.1002/jimd.12069.

An evolutionary approach to optimizing glucose-6-phosphatase-α enzymatic activity for gene therapy of glycogen storage disease type Ia

Lisa Zhang[1], **Jun-Ho Cho**[1], **Irina Arnaoutova**[1], **Brian C. Mansfield**[1,2], and **Janice Y. Chou**[1,*]

[1]Section on Cellular Differentiation, Division of Translational Medicine, Eunice Kennedy Shriver National Institute of Child Health and Human Development, National Institutes of Health, Columbia, MD 21046, USA

[2]Foundation Fighting Blindness, Columbia, MD 21046, USA

Abstract

Glycogen storage disease type-Ia (GSD-Ia), caused by a deficiency in glucose-6-phosphatase-α (G6Pase-α or G6PC), is characterized by impaired glucose homeostasis with a hallmark hypoglycemia, following a short fast. We have shown that *G6pc*-deficient (*G6pc*−/−) mice treated with recombinant adeno-associated virus (rAAV) vectors expressing either wild-type (WT) (rAAV-hG6PC-WT) or codon-optimized (co) (rAAV-co-hG6PC) human (h) G6Pase-α maintain glucose homeostasis if they restore ≥3% of normal hepatic G6Pase-α activity. The codon-optimized vector, which has a higher potency, is currently being used in a phase I/II clinical trial for human GSD-Ia (NCT 03517085). While routinely used in clinical therapies, codon-optimized vectors may not always be optimal. Codon-optimization can impact RNA secondary structure, change RNA/DNA protein binding sites, affect protein conformation and function, and alter post-transcriptional modifications that may reduce potency or efficacy. We therefore sought to develop alternative approaches to increase the potency of the *G6PC* gene transfer vectors. Using an evolutionary sequence analysis, we identified a Ser-298 to Cys-298 substitution naturally found in canine, mouse, rat, and several primate G6Pase-α isozymes, that when incorporated into the WT hG6Pase-α sequence, markedly enhanced enzymatic activity. Using *G6pc*−/− mice, we show that the efficacy of the rAAV-hG6PC-S298C vector was 3-fold higher than that of the rAAV-hG6PC-WT vector. The rAAV-hG6PC-S298C vector with increased efficacy, that minimizes the potential problems associated with codon-optimization, offers a valuable vector for clinical translation in human GSD-Ia.

*Correspondence should be addressed to: Janice Y. Chou, Building 10, Room 8N-240C, NIH, 10 Center Drive, Bethesda, MD 20892-1830, Tel: 301-496-1094; Fax: 301-402-6035, chouja@mail.nih.gov.

Details of the Contributions of Individual Authors:

Lisa Zhang designed and performed the research, analyzed data, and wrote the paper. Jun-Ho Cho and Irina Arnaoutova performed the research and analyzed data. Brian C. Mansfield analyzed data and wrote the paper. Janice Y. Chou designed the research, analyzed data, and wrote the paper.

Conflict of Interest

Lisa Zhang, Jun-Ho Cho, Irina Arnaoutova, Brian C. Mansfield, and Janice Y. Chou declare that they have no conflicts of interest. The Eunice Kennedy Shriver National Institute of Child Health and Human Development has applied patents on the vectors described in this article as an employee invention of Janice Chou.

Animal Rights:

All institutional and national guidelines for the care and use of laboratory animals were followed.

Author Manuscript Author Manuscript Author Manuscript Author Manuscript

Keywords

gene therapy; recombinant adeno-associated virus; glucose-6-phosphatase-α variant; clinical translation for human GSD-Ia; expression optimization

Introduction

Glycogen storage disease type Ia (GSD-Ia, MIM232200) is caused by deleterious mutations in the *G6PC* gene encoding glucose-6-phosphatase-α (G6Pase-α or G6PC) that catalyzes the hydrolysis of glucose-6-phosphate (G6P) to glucose in the terminal step of gluconeogenesis and glycogenolysis (Chou et al 2002, 2010). GSD-Ia patients manifest a phenotype of impaired glucose homeostasis characterized by fasting hypoglycemia, hepatomegaly, nephromegaly, hyperlipidemia, hyperuricemia, lactic acidemia, and growth retardation (Chou et al 2002, 2010). Untreated, GSD-Ia is juvenile lethal. The current dietary therapies have enabled GSD-Ia patients to attain near normal growth and pubertal development, but require strong compliance to a strict diet. However, the underlying pathological processes remain uncorrected and long-term complications including hepatocellular adenoma (HCA), which may undergo transformation to hepatocellular carcinoma (HCC) are common (Chou et al 2002, 2010; Rake et al 2002; Kishnani et al 2014).

Previously, we developed a recombinant adeno-associated virus (rAAV) pseudotype 2/8 vector-mediated gene therapy for GSD-Ia which is currently in clinical trials (NCT 03517085). The trials use rAAV-co-hG6PC (designated as rAAV-co) (Kim et al 2017), a rAAV vector expressing a codon-optimized (co) human (h) *G6PC* cDNA under the control of the h*G6PC* gene promoter/enhancer. During preclinical development of this gene therapy, we had compared constitutive and tissue-specific promoter/enhancers, different AAV serotypes, and *G6PC* wild type (WT) and co-*G6PC* cDNA sequences (Yiu et al 2010; Chou and Mansfield 2011; Lee et al 2012, 2013; Kim et al 2017). We identified a ~2.8-kb h*G6PC* gene promoter/enhancer and showed that regulatory elements contained within this promoter/enhancer are critical for optimal *G6PC* expression in rAAV-mediated gene transfer for GSD-Ia (Lee et al 2013). We further showed that the rAAV-treated mice expressing ≥3% of normal hepatic G6Pase-α activity maintain glucose homeostasis and lack HCA/HCC (Lee et al 2012; Kim et al 2015, 2017). For the clinical trial we chose to use the rAAV-co vector that directed 2–3-fold more hepatic G6Pase-α activity than the rAAV-hG6PC-WT (designed as rAAV-WT) vector at equivalent viral doses (Kim et al 2017). Increasing this activity per dose relationship is valuable for reducing manufacturing costs per human dose, minimizing the viral dose exposure of patients, and reducing the risk of immune responses to the virus.

The codon-optimization of the clinical vector required a 20% change in the native h*G6PC* coding sequence (Kim et al 2017). While codon-optimization is frequently used as a means to improve expression, several studies have noted that such broad changes, while maintaining the protein sequence, can potentially change RNA and DNA protein binding sites, impact RNA secondary structure, affect protein conformation, and even promote resistance to targeted therapy (Stergachis et al 2013; Mauro and Chappell 2014; Bazzini et al

Author Manuscript Author Manuscript Author Manuscript Author Manuscript

2016; Rapino et al 2018). We therefore sought to develop alternative approaches that could improve the expression yet minimize the impact of sequence changes due to broad codon-optimization. The human, dog, mouse, and rat G6Pase-α share 87–91% sequence identity. Intriguingly, *in vitro* expression assays have routinely shown that the canine G6Pase-α isozyme is significantly more active than hG6Pase-α. We therefore expanded our analysis to compare *G6PC* genes across the evolutionary tree, seeking potential codon changes which could enhance enzymatic activity of hG6Pase-α. Here we show that a key residue that impacts enzymatic activity of hG6Pase-α is Ser-298. In canine, mouse, rat and several primate isozymes the corresponding amino acid is a conserved Cys. Introducing this novel change into the WT h*G6PC* gene, to generate hG6Pase-α-S298C, produces an equivalent increase in enzyme activity as the multiple sequence changes required for codon-optimization. Extensive searches of the Exome Aggregation Consortium (ExAC) database for allelic spectrum of *G6PC* have not revealed the S298C as a reported human variant, to date (Lek et al 2016).

We further show that the equivalent rAAV vector, rAAV-hG6PC-S298C (designated as rAAV-S298C) is 3-fold more efficacious than rAAV-WT in directing hepatic G6Pase-α expression in *G6pc*−/− mice, with equivalent efficacy to the rAAV-co vector and offers an attractive second generation vector for clinical translation in GSD-Ia patients.

Materials and methods

Construction of pSVL-hG6Pase-α variants and rAAV-hG6PC vectors

A pSVL vector containing the entire coding region of h*G6PC*-WT cDNA at nucleotides 1 to 1074 was used as a template to produce the human variant constructs, each carrying the selected residue substitution in canine G6Pase-α. A pSVL vector containing the entire coding region of co-h*G6PC* at nucleotides 1 to 1074 (Kim et al 2017) was used as a template to produce the co-hG6PC-S298C construct. For PCR-directed mutagenesis, the template was amplified using two outside PCR primers matching nucleotides 1 to 20 (sense) and 1055 to 1074 (antisense) of the respective cDNA that flanked the sense and antisense variant primers. The hG6Pase-α and co-hG6Pase-α variants were cloned in pSVL and verified by DNA sequencing. The plasmids pTR-GPE-hG6PC (h*G6PC*-WT sequence) and pTR-GPE-co-hG6PC (co-h*G6PC* sequence) have been described (Yiu et al 2010; Kim et al 2017). The pTR-GPE-hG6PC-S298C plasmid was constructed by replacing hG6PC in pTR-GPE-G6PC with the corresponding h*G6PC*-S298C cDNA and the pTR-GPE-co-hG6PC-S298C was constructed by replacing co-hG6PC in pTR-GPE-co-G6PC with the corresponding co-h*G6PC*-S298C cDNA. Both constructs were verified by DNA sequencing. The rAAV-WT, rAAV-S298C, rAAV-co, and rAAV-co-S298C vectors were produced by Vigene Biosciences (Rockville, MD) using the respective pTR plasmids. All 4 vector preparations were further purified and tittered before infusing into 2-week-old *G6pc*−/− mice. Vector purification and tittering were performed by Ultragenyx Pharmaceutical Gene Therapy Division at Cambridge, MA, USA.

Author Manuscript Author Manuscript Author Manuscript Author Manuscript

Expression in COS-1 cells and phosphohydrolase assays

The transfection of a pSVL-hG6Pase-α construct into COS-1 cells and subsequent phosphohydrolase activity assays were as described previously (Shieh et al 2002). Liver microsome isolation and microsomal phosphohydrolase assays were performed as described previously (Lei et al 1996). In phosphohydrolase assays, reaction mixtures (50 μl) containing 50 mM sodium cacodylate buffer, pH 6.5, 2 mM EDTA, 10 mM G6P, and appropriate amounts of microsomal preparations were incubated at 30 °C for 10 min. Disrupted microsomal membranes were prepared by incubating intact membranes in 0.2% deoxycholate for 20 min at 4 °C. Non-specific phosphatase activity was estimated by pre-incubating disrupted microsomal preparations at pH 5 for 10 min at 37 °C to inactivate the acid labile G6Pase-α.

Infusion of *G6pc−/−* mice with rAAV vectors and phenotype analysis

All animal studies were conducted under an animal protocol approved by the Eunice Kennedy Shriver National Institute of Child Health and Human Development Animal Care and Use Committee. The rAAV vector was infused into 2-week-old *G6pc−/−* mice via the retro-orbital sinus as described previously (Yiu et al 2010; Kim et al 2017). Age-matched *G6pc*+/+ and *G6pc*+/− mice with indistinguishable phenotype were used as controls (referred collectively as WT or control mice). Liver samples from WT and rAAV-treated mice were collected at sacrifice following 24-hours of fast. Hepatic levels of glucose, G6P, lactate, and triglyceride were determined as described previously (Kim et al 2015).

Quantification of vector DNA

Total DNA was isolated from liver tissues using the GenElute™ Mammalian Genomic DNA Miniprep Kits (Sigma-Aldrich, St Louis, MO, USA). The vector genome copy numbers were quantified by real-time RT-PCR in an Applied Biosystems 7300 Real-Time PCR System (Foster City, CA) using the forward: 5'-GACCTTTGGTCGCCCGGCCT-3' and reverse: 5'-GAGTTGGCCACTCCCTCTCTGC-3') oligos contained within the inverted terminal repeat of the rAAV vectors. The pTR-GPE-hG6PC plasmid DNA corresponding to 0.01 to 100 copies of the *hG6PC* gene was used in a standard curve.

Quantitative real-time RT-PCR and Western-blot analysis

Total RNA was isolated from liver tissues using the TRIzol Reagent (Invitrogen, Carlsbad, CA, USA). The mRNA expression was quantified by real-time RT-PCR in an Applied Biosystems 7300 Real-Time PCR System using Applied Biosystems TaqMan probes. Data were normalized to Rpl19 RNA. Western-blot images were detected using the LI-COR Odyssey scanner and the Image studio 3.1 software (Li-Cor Biosciences, Lincoln, NE, USA) using mouse monoclonal antibodies against hG6Pase-α (Cho et al 2017) or β-actin (Santa Cruz Biotechnology, Dallas, TX, USA). Protein expression was quantified by densitometry using the Image Studio Lite Ver 5.2 (Li-Cor Biosciences).

Antibodies against hG6Pase-α

Analysis of serum antibodies against human G6Pase-α has been described (Lee et al 2012). Briefly, the Ad-hG6Pase-α infected COS-1 lysates were electrophoresed through a single

Author Manuscript Author Manuscript Author Manuscript Author Manuscript

12% polyacrylamide-SDS gel and transferred onto a PVDF membrane. Membrane strips, representing individual lanes on the gel were individually incubated with the appropriate mouse serum. A monoclonal anti-hG6Pase-α antibody (Cho et al 2017) that also recognizes murine G6Pase-α was used as a positive control.

Statistical analysis

The unpaired t test was performed using the GraphPad Prism Program, version 4 (GraphPad Software, San Diego, CA, USA). Values were considered statistically significant at $p < 0.05$.

Results

Human G6Pase-α variants carrying canine G6Pase-α codon substitutions

In vitro expression assays have revealed that the specific activity of canine G6Pase-α is 4- to 5-fold higher than that of hG6Pase-α. Sequence alignment shows that the 357 amino-acid human and canine G6Pase-α differ in 18 non-conserved residues (Fig. 1). Topological analysis (Pan et al 1998) has shown that hG6Pase-α is anchored in the endoplasmic reticulum (ER) membrane by 9 helices, H1 to H9 creating 4 cytoplasmic (C1 to C4) and 4 luminal (L1 to L4) loops (Fig. 2a). To determine which amino acid substitution results in increased enzymatic activity of canine G6Pase-α, we introduced each selected variant in canine G6Pase-α, singly into the hG6Pase-α-WT sequence, and then determined phosphohydrolase activity of each variant using transient expression assays (Fig. 2b). The results showed that pSVL-hG6Pase-α-S298C (Fig. 2b) carrying a Ser-298 to Cy-298 substitution in H8 is the most active variant. The pSVL-hG6Pase-α-A301V carrying an Ala-301 to Val-301 substitution in H8 was the second most active variant (Fig. 2b). However, the dual variant pSVL-hG6Pase-α-S298C/A301V exhibited similar phosphohydrolase activity as the pSVL-hG6Pase-α-S298C single variant (Fig. 2b) and was not characterized further.

Sequence alignment across the evolutionary tree shows that Cys-298 is an allele found in canine, mouse, rat and several primate G6Pase-α isozymes (Fig. 1). We have previously generated co-hG6Pase-α and showed that pSVL-co-hG6Pase-α directed significantly higher phosphohydrolase activity than pSVL-hG6Pase-α-WT (Kim et al 2017). Here transient expression assays showed that phosphohydrolase activities of pSVL-hG6Pase-α-S298C, pSVL-co-hG6Pase-α, and pSVL-co-hG6Pase-α-S298C, which combines codon optimization with the S298C variant in the same construct, were 1.7-, 1.6-, and 2.8-fold higher, respectively than that of the pSVL-hG6Pase-α-WT construct (Fig. 3a).

Studies have shown that codon-optimization improves protein expression (Inouye et al 2015). Supporting this, transient expression assays showed that the pSVL-co-hG6Pase-α construct directed the synthesis of 1.7-fold higher levels of the hG6Pase-α protein than the pSVL-hG6Pase-α-WT construct (Fig. 3b). Interestingly, the pSVL-hG6Pase-α-S298C and pSVL-co-hG6Pase-α-S298C constructs directed the synthesis of 1.9- and 3.7-fold higher levels of hG6Pase-α, respectively as compared to the pSVL-hG6Pase-α-WT construct (Fig. 3b), indicating that the Ser-298 to Cys-298 substitution in hG6Pase-α stabilized the enzyme.

Author Manuscript Author Manuscript Author Manuscript Author Manuscript

The rAAV-S298C vector exhibits increased efficacy in *G6pc−/− mice*

To select the most efficacious vectors for clinical translation, we generated rAAV-S298C, a rAAV vector expressing the hG6Pase-α-S298C variant. Because of the markedly high phosphohydrolase activity exhibited by the pSVL-co-hG6Pase-α-S298C construct, we also generated AAV-co-S298C, a rAAV vector expressing the co-hG6Pase-α-S298C variant. Two-week-old *G6pc−/−* mice were treated with 10^{12} vp/kg of rAAV-S298C and AAV-co-S298C compared to mice treated with either rAAV-WT or rAAV-co as controls. At age 4 weeks, hepatic G6Pase-α activities in rAAV-S298C-, rAAV-co-, and rAAV-co-S298C-treated *G6pc−/−* mice were 2.9-, 2.7-, and 4.8-fold higher, respectively than that in rAAV-WT-treated mice (Fig. 3c), confirming the *in vitro* expression results. As noted in earlier studies, the expression of rAAV-mediated G6Pase-α expression decreased during postnatal development (Yiu et al 2010). Hepatic G6Pase-α activities in the 10^{12} vp/kg of rAAV-treated mice decreased from age 4 to age 12 weeks: rAAV-WT decreased by 4.8 fold (16.0 ± 4.4 to 3.3 ± 0.4 nmol/min/mg); rAAV-S298C decreased by 4.5 fold (45.8 ± 7.1 to 10.2 ± 1 nmol/min/mg); rAAV-co decreased by 5.3 fold (42.6 ± 6.8 to 8.0 ± 1 nmol/min/mg); and rAAV-co-S298C decreased by 6.1 fold (77.0 ± 5.2 to 12.7 ± 3 nmol/min/mg) (Fig. 3c). The 4.5 to 6.1-fold loss in hepatic G6Pase-α activity from age 4 to 12 weeks reflects the loss of episomal rAAV vector, resulting from the fast rate of hepatocellular proliferation during early postnatal mouse development (Yiu et al 2010). It is notable that while combining codon optimization with the S298C variant in the same vector increased initial expression, there was a greater fold loss over time, resulting in not significant overall benefit over the rAAV-S298C or rAAV-co vector by age 12 weeks.

We then compared vector copy numbers per diploid genome in the 10^{12} vp/kg rAAV-treated animals at age 12 weeks when postnatal mitosis associated with liver growth has stopped. Significantly, the values of vector copy numbers/diploid genome varied only slightly among the 4 vectors (Fig. 3d), confirming a dosage uniformity. To partly offset this initial drop in expression when treating very young mice, we increased the dosage for 2-week-old *G6pc−/−* mice 10-fold to10^{13} vp/kg for subsequent studies. Again, at age 12 weeks, the values of vector copy numbers/diploid genome varied only slightly among the 4 vectors (Fig. 3d). The mean hepatic microsomal G6Pase-α activity of 12-week-old control mice was 258.5 ± 13 nmol/min/mg. At age 12 weeks, hepatic microsomal G6Pase-α activity in mice infused at age 2 weeks with 10^{13} vp/kg of the respective vectors were 58.8 ± 8.5 (rAAV-WT), 195.3 ± 27.6 (rAAV-S298C), 196.7 ± 13.9 (rAAV-co), and 221.9 ± 22.1 (rAAV-co-S298C) nmol/min/mg (Fig. 3e). It is interesting to note that at age 12 weeks, hepatic microsomal G6Pase-α activity in 2-week-old *G6pc−/−* mice treated with 10^{13} vp/kg of rAAV-S298C, rAAV-co, and rAAV-co-S298C were 3.3-, 3.3-, and 3.4-fold higher, respectively than the rAAV-WT-treated mice (Fig. 3e). Again, the initial efficacy advantage of the rAAV-co-S298C vector diminished with time *in vivo*. We therefore performed phenotype analysis primarily in the rAAV-S298C-treated *G6pc*−/− mice.

Phenotype of 12-week-old rAAV-treated mice

The hallmark of GSD-Ia is fasting hypoglycemia (Chou et al 2002, 2010). At age 12 weeks, all *G6pc*−/− mice treated with either 10^{12} vp/kg or 10^{13} vp/kg of the rAAV-WT, rAAV-S298C, and rAAV-co vectors could tolerate 24 hours of fast (Fig. 3f). Consistent with levels

Author Manuscript Author Manuscript Author Manuscript Author Manuscript

of G6Pase-α activity restored, fasting glucose levels in mice treated with 10^{12} vp/kg were significantly lower than the levels in control mice (Fig. 3f). Notably the cohort treated with 10^{13} vp/kg had a fasting glucose profile very similar to that of the control mice (Fig. 3f).

We have previously shown that the rAAV-WT- and rAAV-co-treated *G6pc*−/− mice expressing ≥3% of normal hepatic G6Pase-α activity maintain glucose homeostasis and are protected against age-related obesity (Lee et al 2012; Kim et al 2015, 2017). At age 12 weeks, the average body weight (BW) values of rAAV-treated *G6pc*−/− mice at either dosage were lower than those of their age-matched control mice (Fig. 4a), suggesting that the rAAV-S298C-treated *G6pc*−/− mice were also leaner. GSD-Ia is characterized by hepatomegaly. Compared to control mice at age 12 weeks, the ratios of liver weight (LW) to BW were markedly higher in rAAV-treated mice (Fig. 4b). However, when absolute LW values were compared directly, there was no significant difference between control and *G6pc*−/− mice treated with 10^{13} vp/kg of either the rAAV-S298C or the rAAV-co vector (Fig. 4b). The mice treated with rAAV-WT at 10^{13} vp/kg, however, continued exhibiting hepatomegaly.

During fasting, blood glucose homeostasis is maintained by endogenous glucose produced in the liver by the G6Pase-α/G6P transporter (G6PT) complex (Chou et al 2002, 2010). The G6PT transports G6P from the cytoplasm into the ER lumen and G6Pase-α, with its active site inside the lumen (Pan et al 1998), hydrolyzes intraluminal G6P to glucose. When G6Pase-α is downregulated, the expression of G6PT is enhanced to compensate for the decrease in G6Pase-α activity (Lee et al 2012). After 24 hours of fast, hepatic glucose levels in 12-week-old control mice averaged 208.6 ± 6.4 nmol/mg protein (Fig. 4c). The 24 hour-fasted hepatic glucose levels in 12-week-old mice treated with 10^{12} vp/kg of rAAV-WT, rAAV-S298C and rAAV-co were 24%, 32%, and 32%, respectively of the control levels (Fig. 4c). This suggests that 24% of normal hepatic glucose levels was sufficient to maintain blood glucose homeostasis during a long fast. At age 12 weeks, the 24 hour-fasted hepatic glucose levels in mice treated with 10^{13} vp/kg of the respective vectors were indistinguishable from the levels in the control mice (Fig. 4c). As expected, hepatic levels of *G6pt* mRNA in 10^{12} vp/kg and 10^{13} vp/kg rAAV-treated *G6pc*−/− mice were markedly increased over those of control mice (Fig. 4d), confirming earlier studies showing a feedback response which increases the expression of *G6pt* mRNA to offset the lower G6Pase-α activity (Lee et al 2012).

While hepatic G6P and triglyceride contents in 10^{12} vp/kg rAAV-treated mice were significantly higher than those in the control mice, administering a 10-fold higher dose (10^{13} vp/kg) of these rAAV vectors, normalized both G6P and triglyceride contents (Fig. 4e). Hepatic lactate contents in 10^{12} vp/kg and 10^{13} vp/kg rAAV-treated mice were significant higher than that in control mice, although the increase was less pronounced in the higher dose rAAV-treated mice (Fig. 4e).

To determine whether a humoral response directed against human G6Pase-α was generated in the infused mice, we performed Western-blot analysis of sera obtained from 12- week-old G6pc−/− mice infused at age 2 weeks with 10^{13} vp/kg of rAAV-WT, rAAV-S298C, or rAAV-co, using a monoclonal anti-hG6Pase-α antibody (Cho et al 2017) as a positive control. We

Author Manuscript Author Manuscript Author Manuscript Author Manuscript

detected no antibodies against human G6Pase-α in the sera of control (+/+), rAAV-WT-, rAAV-S298C-, and rAAV-co-treated mice (Fig. 4f).

Discussion

Previous long-term studies have shown that *G6pc*−/− mice treated with rAAV-WT or rAAV-co, tittered to restore 3–63% of normal hepatic G6Pase-α activity, maintain glucose homeostasis and do not develop HCA/HCC (Lee et al 2012; Kim et al 2015, 2017). We have also shown that the rAAV-co vector, selected for the phase I/II clinical trial for human GSD-Ia (NCT03517085), is more efficacious in restoring hepatic G6Pase-α expression than the rAAV-WT vector (Kim et al 2017). Studies have shown that the broad change in sequence during codon-optimization could impact RNA secondary structure, change RNA/DNA protein binding sites, and affect protein conformation (Stergachis et al 2013; Mauro and Chappell 2014; Bazzini et al 2016; Rapino et al 2018). The impact of those changes might have to a therapeutic is not clear. However, any less intrusive change in the coding sequence, that can bring the same benefit as codon-optimization, may be a useful alternative. In this study, we report a novel hG6PC-S298C variant having only a 2-bp (0.2%) change to the h*G6PC*-WT coding sequence that confers a similar benefit as the fully codon-optimized vector. The gene transfer studies in *G6pc*−/− mice showed that rAAV-S298C and rAAV-co vectors have similar efficacy, both being ~3-fold more efficacious in directing hepatic G6Pase-α expression than the rAAV-WT vector. Moreover, we detected no antibodies against human G6Pase-α in the sera of rAAV-WT-, rAAV-S298C-, or rAAV-co-treated *G6pc*−/− mice. Collectively, the rAAV-S298C vector with minimal change in the native coding sequence, yet delivering the same benefits as the codon-optimization strategy offers a vector of choice for clinical translation in human GSD-Ia.

We also examined whether combining codon optimization with the S298C variant in the same construct could yield a more active vector. Transient expression assays showed that phosphohydrolase activity directed by the pSVL-co-G6Pase-α-S298C construct was the highest, being 2.8-fold higher than that of the pSVL-hG6Pase-α-WT construct. Compared to rAAV-WT-treated *G6pc*−/− mice, hepatic G6Pase-α activities in *G6pc*−/− mice transduced with 10^{12} vp/kg of rAAV-S298C, rAAV-co, or rAAV-co-S298C were 2.9-, 2.7-, and 4.8-fold higher, respectively at age 4 weeks and were 3.1-, 2.4-, and 3.8-fold higher, respectively at age 12 weeks. Notably, hepatic G6Pase-α expression in *G6pc*−/− mice directed by the rAAV-co-S298C vector decreased more rapidly with time. Interestingly, at age 12 weeks, hepatic G6Pase-α activities in mice infused at age 2 weeks with 10^{13} vp/kg of rAAV-S298C, rAAV-co, and rAAV-co-S298C vectors were similar, being ~3-fold higher than the mice infused with 10^{13} vp/kg of rAAV-WT. The reason for the larger decline in transgene expression directed by the rAAV-co-S298C vector is currently unclear. We plan to compare these 4 vectors in a long-term efficacy study.

Human G6Pase-α is an intracellular enzyme anchored in the ER membrane by 9 helices (Fig. 2a) (Pan et al 1998). Structure-function studies of hG6Pase-α have shown that the structural integrity of the transmembrane helices is important for enzyme activity (Shieh et al 2002). In this study, we show that the hG6Pase-α-S298C variant harboring a Ser-298 to Cys-298 substitution in H8 that is conserved in dog, rat, mice, and several primates,

Author Manuscript Author Manuscript Author Manuscript Author Manuscript

displayed increased enzyme stability and activity, although this variant has not been reported to date in human gene databases. Amino acid sequences within H8 of G6Pase-α appear to be critical to the overall enzyme activity. While S298C increases specific enzyme activity, other mutations, such as the naturally occurring human GSD-Ia mutations, R295C and S298P inactivate the hG6Pase-α enzyme (Shieh et al 2002). The introduction of a Cys residue raises the question of whether there is a new disulfide bond in the enzyme that can increase protein stability and/or activity (Trivedi et al 2009). There are 7 Cys residues in hG6Pase-α-WT and 8 Cys residues in the hG6Pase-α-S298C variant (Fig. 2a). Prediction using *in silico* analysis (http://scratch.proteomics.ics.uci.edu/index.html) has identified a new disulfide bond spanning H8 (Cys-298) and C4 (Cys-284). One speculative possibility, given such a bond is between a membrane localized residue and a cytoplasmic one, is that a conformational change mediated by the newly introduced disulfide bond in the hG6Pase-α-S298C variant increases the stability and/or activity of the isozyme.

To date, hG6PC-expressing rAAV vectors of different serotypes have been used to treat canine GSD-Ia (Weinstein et al 2010; Demaster et al 2012). In contrast to mouse studies requiring only a single rAAV infusion, gene transfer efficacy in GSD-Ia dog usually waned, and to maintain glucose homeostasis of the treated dogs, it was necessary to re-administer a new rAAV-hG6PC of different serotypes. The finding that the canine G6Pase-α is significantly more active than the human isozyme may suggest a higher level of G6Pase-α activity is required in other species and this may provide an explanation why gene therapy studies using the human *G6PC* gene in GSD-Ia dogs are less effective. This suggests that the efficacy of gene therapy in GSD-Ia dogs would be improved if a canine G6Pase-α-expressing rAAV vector is used.

In summary, we show that the rAAV-S298C vector is 3-fold more efficacious in directing hepatic G6Pase-α expression than the rAAV-WT vector. The rAAV-S298C vector with increased efficacy and devoid of potential problems associated with codon-optimization offers a valuable second generation vector for clinical translation in human GSD-Ia.

Funding

This research was supported by the Intramural Research Program of the Eunice Kennedy Shriver National Institute of Child Health and Human Development, National Institutes of Health.

Abbreviations

AAV	adeno-associated virus
co	codon-optimized
ER	endoplasmic reticulum
G6P	glucose-6-phosphate
G6Pase-α	glucose-6-phosphatase-α
G6PT	glucose-6-phosphate transporter

Author Manuscript Author Manuscript Author Manuscript Author Manuscript

GSD-Ia	glycogen storage disease type Ia
HCA	hepatocellular adenoma
HCC	hepatocellular carcinoma
WT	wild-type

References

Bazzini AA, Del Viso F, Moreno-Mateos MA et al. (2016) Codon identity regulates mRNA stability and translation efficiency during the maternal-to-zygotic transition. EMBO J 35: 2087–2103 [PubMed: 27436874]

Cho JH, Kim GY, Pan CJ et al. (2017) Downregulation of SIRT1 signaling underlies hepatic autophagy impairment in glycogen storage disease type Ia. PLoS Genet 13: e1006819 [PubMed: 28558013]

Chou JY, Jun HS, Mansfield BC (2010) Glycogen storage disease type I and G6Pase-beta deficiency: etiology and therapy. Nat Rev Endocrinol 6: 676–688 [PubMed: 20975743]

Chou JY, Mansfield BC (2011) Recombinant AAV-directed gene therapy for type I glycogen storage diseases. Expert Opin Biol Ther 11: 1011–1024 [PubMed: 21504389]

Chou JY, Matern D, Mansfield BC, Chen YT (2002) Type I glycogen storage diseases: disorders of the glucose-6-phosphatase complex. Curr Mol Med 2: 121–143 [PubMed: 11949931]

Demaster A, Luo X, Curtis S et al. (2012) Long-term efficacy following readministration of an adeno-associated virus vector in dogs with glycogen storage disease type Ia. Hum Gene Ther 23: 407–418 [PubMed: 22185325]

Inouye S, Sahara-Miura Y, Sato J, Suzuki T (2015) Codon optimization of genes for efficient protein expression in mammalian cells by selection of only preferred human codons. Protein Expr Purif 109: 47–54 [PubMed: 25665506]

Kim GY, Lee YM, Cho JH et al. (2015) Mice expressing reduced levels of hepatic glucose-6-phosphatase-α activity do not develop age-related insulin resistance and obesity. Hum Mol Genet 24: 5115–5125 [PubMed: 26089201]

Kim GY, Lee YM, Kwon JH et al. (2017) Glycogen storage disease type Ia mice with less than 2% of normal hepatic glucose-6-phosphatase-α activity restored are at risk of developing hepatic tumors. Mol Genet Metab 120: 229–234 [PubMed: 28096054]

Kishnani PS, Austin SL, Abdenur JE et al. (2014) Diagnosis and management of glycogen storage disease type I: a practice guideline of the American College of Medical Genetics and Genomics. Genet Med 16:e1 [PubMed: 25356975]

Lee YM, Jun HS, Pan CJ et al. (2012) Prevention of hepatocellular adenoma and correction of metabolic abnormalities in murine glycogen storage disease type Ia by gene therapy. Hepatology 56: 1719–1729 [PubMed: 22422504]

Lee YM, Pan CJ, Koeberl DD, Mansfield BC, Chou JY (2013) The upstream enhancer elements of the G6PC promoter are critical for optimal G6PC expression in murine glycogen storage disease type Ia. Mol Genet Metab 110: 275–280 [PubMed: 23856420]

Lei KJ, Chen H, Pan CJ et al. (1996) Glucose-6-phosphatase dependent substrate transport in the glycogen storage disease type-1a mouse. Nat Genet 13(2): 203–209 [PubMed: 8640227]

Lek M, Karczewski KJ, Minikel EV et al. (2016) Analysis of protein-coding genetic variation in 60,706 humans. Nature 536: 285–291 [PubMed: 27535533]

Mauro VP, Chappell SA (2014) A critical analysis of codon optimization in human therapeutics. Trends Mol Med 20: 604–613 [PubMed: 25263172]

Pan CJ, Lei KJ, Annabi B, Hemrika W, Chou JY (1998) Transmembrane topology of glucose-6-phosphatase. J Biol Chem 273: 6144–6148 [PubMed: 9497333]

Rake JP, Visser G, Labrune P, Leonard JV, Ullrich K, Smit GP (2002) Glycogen storage disease type I: diagnosis, management, clinical course and outcome. Results of the European Study on Glycogen Storage Disease Type I (ESGSD I). Eur J Pediat 161: S20–S34

Author Manuscript Author Manuscript Author Manuscript Author Manuscript

Rapino F, Delaunay S, Rambow F et al. (2018) Codon-specific translation reprogramming promotes resistance to targeted therapy. Nature 558: 605–609 [PubMed: 29925953]

Shieh JJ, Terzioglu M, Hiraiwa H et al. (2002) The molecular basis of glycogen storage disease type 1a: structure and function analysis of mutations in glucose-6-phosphatase. J Biol Chem 277: 5047–5053 [PubMed: 11739393]

Stergachis AB, Haugen E, Shafer A et al. (2013) Exonic transcription factor binding directs codon choice and affects protein evolution. Science 342: 1367–1372 [PubMed: 24337295]

Trivedi MV, Laurence JS, Siahaan TJ (2009) The role of thiols and disulfides on protein stability. Curr Protein Pept Sci 10: 614–625 [PubMed: 19538140]

Weinstein DA, Correia CE, Conlon T et al. (2010) Adeno-associated virus-mediated correction of a canine model of glycogen storage disease type Ia. Hum Gene Ther 21: 903–910l. [PubMed: 20163245]

Yiu WH, Lee YM, Peng WT et al. (2010) Complete normalization of hepatic G6PC deficiency in murine glycogen storage disease type Ia using gene therapy. Mol Ther 18:1076–1084 [PubMed: 20389290]

Author Manuscript Author Manuscript Author Manuscript Author Manuscript

Synopsis:

A human *G6PC* gene transfer vector expressing a novel human G6PC-S298C variant, designed using an evolutionary analysis of *G6PC* genes, displays 3-fold higher activity than the vector encoding the wild-type human *G6PC* protein and offers an attractive second generation vector for clinical translation in GSD-Ia patients.

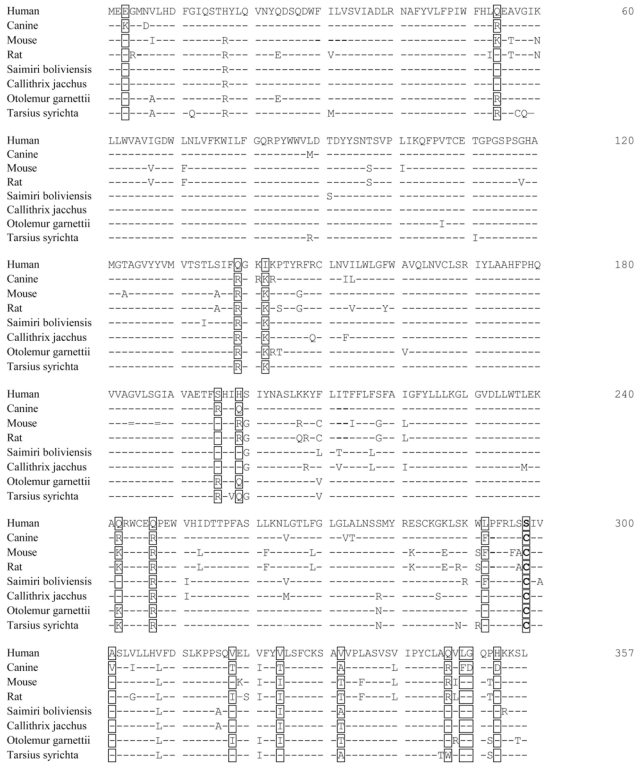

Fig. 1.

Alignment of the amino acid sequences of mammalian G6Pase-α. The non-conserved amino acids between human and canine G6Pase-α are bracketed. The G6Pase-α sequences are GENBANK accession numbers U01120 (human), U91844 (dog), U00445 (mouse), U07993 (rat), XP_003942781 (Saimiri boliviensis), XP_002748054 (Callithrix jacchus), XP_003786361 (Otolemur garnettii), and XP_008066427 (Carlito syrichta).

Author Manuscript Author Manuscript Author Manuscript Author Manuscript

Author Manuscript Author Manuscript Author Manuscript Author Manuscript

a

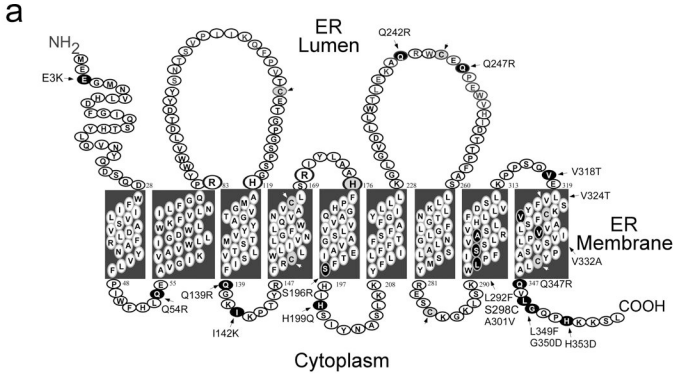

b

pSVL-hG6Pase-α constructs	Phosphohydrolase activity nmol/min/mg	pSVL-hG6Pase-α constructs	Phosphohydrolase activity nmol/min/mg
WT	154.5 ± 9.5		
p.E3K (N-terminal)	145.9 ± 3.5	**p.S298C (H8)**	**341.4 ± 16.4** (2.2-fold)
p.Q54R (C1)	159.6 ± 7.3	p.A301V (H8)	211.7 ± 12.5 (1.4-fold)
p.Q139R (C2)	103.1 ± 6.7	p.V318T (L4)	146.7 ± 16.3
p.I142K (C2)	131.0 ± 4.4	p.V324T (H9)	107.6 ± 8.2
p.S196R (H5)	80.5 ± 2.5	p.V332A (H9)	150.5 ± 13.1
p.H199Q (C3)	144.0 ± 7.4	p.Q347R (C-terminal)	152.5 ± 7.9
p.Q242R (L3)	164.5 ± 4.0	p.L349F (C-terminal)	176.4 ± 5.9
p.Q247R (L3)	133.8 ± 16.4	p.G350D (C-terminal)	136.6 ± 16.7
p.L292F (H8)	130.3 ± 20.3	p.H353D (C-terminal)	154.7 ± 2.8
		p.S298C/p.A301V (H8)	**343.7 ± 18.8** (2.2-fold)

Fig. 2.

Characterization of pSVL-hG6Pase-α variants harboring the non-conserved amino acids in canine G6Pase-α. (**a**) The hG6Pase-α enzyme is anchored in the ER membrane by 9 helices (H1 to H9), creating 4 cytoplasmic (C1 to C4) and 4 luminal (L1 to L4) loops. The amino-terminus is located in the ER lumen and the carboxyl-terminus in the cellular cytoplasm. The non-conserved amino acids in hG6Pase-α differing from that in canine G6Pase-α are indicated and shown in black. The Cys residues are shown in grey and indicated by arrow heads. (**b**) Phosphohydrolase activity of WT and variant hG6Pase-α after transfecting of the pSVL constructs into COS-1 cells. Numbers in parenthesis represent fold increase in phosphohydrolase activity over the WT construct. Data represent the mean ± SEM. *$p <$ 0.05, **$p < 0.005$.

Author Manuscript Author Manuscript Author Manuscript Author Manuscript

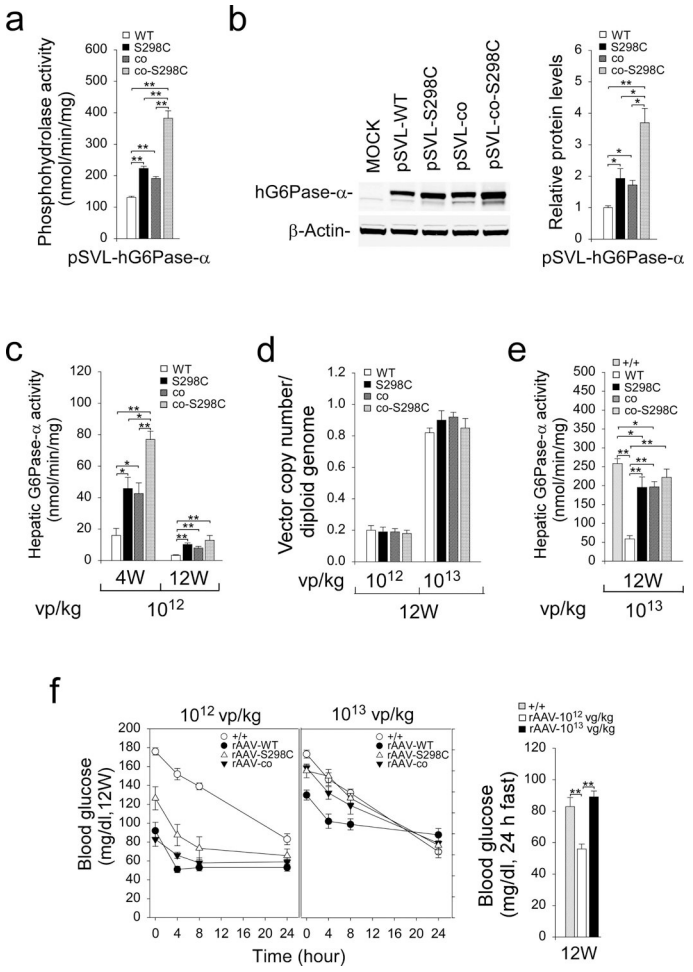

Fig. 3.

Transient expression assays of G6Pase-α constructs and phenotype analyses of rAAV-treated *G6pc*−/− mice. (**a**) Phosphohydrolase activity after transfecting the pSVL-hG6Pase-α-WT, pSVL-hG6Pase-α-S298C, pSVL-co-hG6Pase-α, or pSVL-co-hG6Pase-α-S298C construct into COS-1 cells. (**b**) Western-blot analysis of hG6Pase-α and β-actin after transient expression of the pSVL-hG6Pase-α-WT, pSVL-hG6Pase-α-S298C, pSVL-co-hG6Pase-α, pSVL-co-hG6Pase-α-S298C construct into COS-1 cell along with quantification by densitometry (n = 3). (**c**-**f**) Phenotypic analyses of rAAV-treated *G6pc*−/− mice. Two-week-old *G6pc*−/− mice were treated with 10^{12} or 10^{13} vp/kg of rAAV-WT (n = 12), rAAV-S298C (n = 12), rAAV-co (n = 12), or rAAV-co-S298C (n = 12) vector, and phenotype analyzed at age 4 weeks (6 mice/treatment) and 12 weeks (6 mice/treatment). (**c**) Hepatic microsomal G6Pase-α activity in mice treated with the rAAV vectors at 10^{12} vp/kg. (**d**) Vector genome copy numbers in the livers of 12-week-old mice. (**e**) Hepatic microsomal G6Pase-α activity in mice treated with the rAAV vectors at 10^{13} vp/kg. (**f**) Fasting blood glucose tolerance profiles and blood glucose levels following a 24-hour of fast. Data represent the mean ± SEM. *$p < 0.05$, **$p < 0.005$.

Author Manuscript Author Manuscript Author Manuscript Author Manuscript

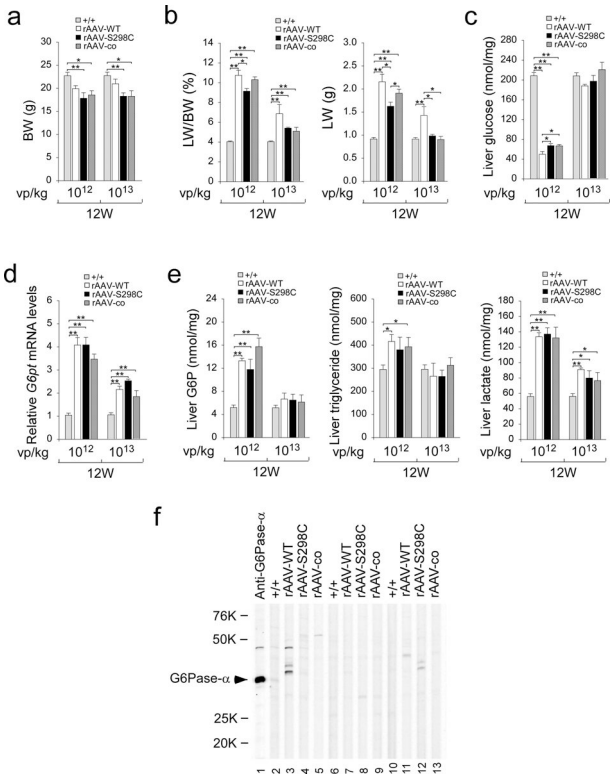

Fig. 4.

Phenotypic analyses of rAAV-treated *G6pc*−/− mice at age 12 weeks. *G6pc*−/− mice were treated at age 2 weeks with either 10^{12} vp/kg or 10^{13} vp/kg of rAAV-WT, rAAV-S298C, or rAAV-co, and analyzed at age 12 weeks. The data were obtained from WT (+/+, n = 12) and *G6pc*−/− mice treated with either 10^{12} vp/kg (n = 6 per vector) or 10^{13} vp/kg (n = 6 per vector) of rAAV-WT, rAAV-S298C, or rAAV-co. (**a**) BW. (**b**) LW/BW ratios and LW. (**c**) Hepatic glucose levels. (**d**) Relative *G6pt* mRNA levels. (**e**) Hepatic levels of G6P, triglyceride, and lactate. (**f**) Western-blot analysis of serum antibodies against human G6Pase-α. The serum samples were obtained from 12 week-old *G6pc*−/− mice treated at age 2 weeks with 10^{13} vp/kg of rAAV-WT, rAAV-S298C, or rAAV-co vector. Lanes 1: anti-hG6Pase-α antiserum; lanes 2, 6, 10: serum samples (1: 50 dilution) from WT mice; lanes 3, 7, 11: serum samples (1: 50 dilution) from rAAV-WT-treated *G6pc*−/− mice; lanes 4, 8, 12: serum samples (1: 50 dilution) from rAAV-S298C-treated *G6pc*−/− mice; and lanes 5, 9, 13: serum samples (1: 50 dilution) from rAAV-co-treated *G6pc*−/− mice. Data represent the mean ± SEM. *$p < 0.05$, **$p < 0.005$.